



## IDENTIFICATION OF BUILDING DAMAGE USING ARMAX MODEL: A PARAMETRIC STUDY

Tarek Edrees SAAED <sup>a), b)</sup>, George NIKOLAKOPOULOS <sup>c)</sup>

<sup>a)</sup> Department of Civil, Environmental and Natural Resources Engineering, Division of Structural and Construction Engineering, Luleå University of Technology, Luleå, Sweden, e-mail: [tarek.edrees@ltu.se](mailto:tarek.edrees@ltu.se),

<sup>b)</sup> Lecturer at University of Mosul, College of Engineering, Department of Civil Engineering, Iraq, e-mail: [tareked970@gmail.com](mailto:tareked970@gmail.com)

<sup>c)</sup> Department of Computer Science, Electrical and Space Engineering, Division of Systems and Interaction, Luleå University of Technology, Luleå, Sweden, e-mail: [geonik@ltu.se](mailto:geonik@ltu.se)

### Summary

The Structural Identification approach is used to identify and localize the existence of damage for a steel frame. The black box linear parametric model called Auto-Regressive Moving Average with eXternal input (ARMAX) was utilized for the construction of the Frequency Response Functions, based on simulation results. The Singular Value Decomposition method was adopted to identify how many significant eigenvalues exist and plot the Complex Mode Indicator Function for the complete frame. Three damage indices were adopted to evaluate the state of damage in the frame. The results indicated that the ARMAX is a robust scheme for structural damage detection.

Keywords: Structural Identification; Damage Detection; Non-Destructive Evaluation; ARMAX model; Structural Dynamic.

## 1. INTRODUCTION

The Finite-Element (FE) and the experimental modal analysis methods have been intensively used for a long time as a tool for the weakness assessment and rehabilitation for civil engineering structures. However, it has been increasingly recognized that a FE model developed from design drawings, has many probable error sources like: discretization, geometric, numerical computation, shape function, geometry of various finite elements, insufficient representation of structural systems, boundary and continuity conditions, and material properties and their variations [36]. Moreover, the ever-growing complexity of structures and the use of new construction materials impose more limitations on the finite-element model's accuracy. Many examples showed that the difference between the simulated and measured responses may be reach up to 500% and 100% for local and global responses respectively, because the refined finite-element model of a structure is still affected by the approximation and finite-element assumptions [10]. Furthermore, owing to the cost considerations, there is an urgent need for sufficient and reliable methods for evaluating the real conditions of aged infrastructures in order to take the optimal decisions concerning their rehabilitation, and thus, the need for Test-validated finite-element models is crucial in order to secure the required performance and reliability [36, 2].

Moreover, the general trend in civil engineering nowadays is to evolve from specification-based to performance-based engineering due to many

reasons, such as the extreme loading events like earthquakes, hurricanes, and floods, which call for a continuous improvement of design methods and procedures [1]. Comprehensive information about the early start of structural identification and the first contributions until 1971 were presented by [4], who discussed thoroughly the methods for identification of linear, non-linear systems and real time identification methods. One of the important contributions of system identification was done by [18], who firstly, introduced the concept to the engineering mechanics' researchers and then introduced it to structural engineers by presenting and formulating the problem of system identification. Furthermore, they proposed the probable application of different testing procedures and the potential practical implementation of system identification method for damage detection [23]. According to [10], system identification can be utilized to fulfill different investigation goals, for instance: (1) design verification and construction planning, (2) means of measurement-based delivery of a design-build contract, (3) document as-is structural characteristics to serve as a baseline for assessing any future changes, (4) Load-capacity rating for inventory or special permits, (5) evaluate possible performance deficiency's causes, (6) evaluate reliability and vulnerability, (7) designing structural modification and retrofit or hardening, (8) health and performance monitoring, (9) asset management based on benefit/cost, and (10) to help the civil engineers for better understanding of how actual structural systems are loaded.

Nowadays, applications of system identification in civil engineering are widely spread, especially in the field of damage detection, while the overall aim of this article is to utilize the black box linear parametric model called Auto-Regressive Moving Average with eXternal input ARMAX model for damage identification and localization. The importance of the ARMAX models employed in the current study and in comparison with the ARMA models utilized so far in the related literature, comes from the following facts: 1) the ARMAX model structure involves disturbance dynamics and have more flexibility in the handling of disturbance modeling than the other parametric stochastic time series models because they offer to model deterministic and stochastic parts of the system independently, 2) they are helpful when the dominating disturbances enter early in the process (for instance, at the input), 3) the ARMAX model structure relies not only on the present value of the input and output, but the history of both, and 4) it introduces several different variants and techniques available to handle a variety of cases [33, 34]. Thus, the contribution of this article is to assist in a better understanding of the potentials of using ARMAX modelling, while proposing a novel strategy by combining this approach with the utilization of the SVD and the CMIF curves based techniques in the damage detection of structures, and thus clarifying to what extent damages in a multi-story steel building can be identified by evaluating the changes in the modal parameters. The novel proposed methodology, for evaluating the damage detection, is based on the following procedures: a) implementing an ARMAX model for predicting the Frequency Response Functions (FRF), b) constructing the mobility matrix (H) from the predicted FRF and utilizing them for damage identification and localization.

For instance, Mitsuru et al. demonstrated the efficiency of using a neural network-based approach to detect damage in a steel building in Japan [32]. Capecchi & Vestroni studied the monitoring of structural systems by using frequency data and clarify when it is enough to measure natural frequencies only or natural frequencies and modal shapes to detect damage [8, 47] outlined a statistical method with combined uncertain frequency and mode shape data for structural damage identification, and their experimental tests proved the efficiency of this method to detect damage existence. Li et al. [22] utilized empirical mode decomposition and wavelet analysis for damage detection of a 4-storey shear building model. da Silva et al. [13] used fuzzy clustering method for classification of structural damage. Valuable information about system identification and its applications in damage detection are presented by Nagarajaiah. Furthermore, Nagarajaiah and coworkers developed a new interaction matrix formulation and input error formulation to detect the presence of damage in the structural member up to

level 4 (discover the extent of damage) [32]. Hilbert-Huang transform was used to detect damage in benchmark buildings [44] and for experimental identification of bridge health, under ambient vibrations [24, 25].

Additionally, [21] estimated only the modal parameters using ARMAX models. Vector ARMA models were utilized by Andersen [3] for identification of civil engineering structures. Bodeux and Golinval [6] used the Auto-Regressive Moving Average Vector (ARMAV) model for system identification and damage detection of buildings. [48] proposed a substructure approach based on ARMAX model that permits for the local damage detection of a shear structure. Minami et al. [29] utilized an ARX model for system identification of super high-rise buildings using limited vibrations data. [28] implemented the recursive stochastic subspace identification method to identify the time-varying dynamic properties of the mid-story isolation building by utilizing ambient vibration test data, while the recursive subspace identification method was used for the same purpose by utilizing the earthquake response data.

Kampas and Makris [20] applied the Parameter Estimating Method (PEM) to identify the modal characteristics (damping and frequency) of a bridge, compared the results with the previous studies, and concluded that the linear models are able to fit the measured responses. Furthermore, a comprehensive overview of the system identification principles, recent developments and typical case studies for successful applications of system identification to constructed buildings around the world are well documented in [10].

Despite the enormous developments in parametric model's identification methods, their relative merits and performance as correlated to the vibrating structures are still incomplete. The reason for this limited knowledge is due to the lack of comparative studies under various test conditions [37] and the lack of extended applications of these methods with real life data. In the present work, the Structural Identification approach is used to identify the existence of damage and damage locations for a bench mark steel building's frame. The ARMAX modeling was utilized for the construction of FRF based on simulation results. Abaqus 6.12 finite-element software was utilized to perform the time history analysis for the case under study and the obtained responses at 110 different locations (assumed as a sensors) correspond to the ends of columns and mid of beams were further processed by the parametric models to obtain the building's FRFs based on the Abaqus analysis results (assumed as measurements).

The damage in the frame was simulated by reducing the modulus of elasticity (E) for specific columns by 75% of the undamaged ones. Two damage scenarios were assumed for damages in the frame. Damage scenario no.1 consist of increasingly destroying the columns of the ground floor, while

for the damage scenario no.2, the damage locations were changed by destroying column no.1 in a floor, and this was repeated for five stories. The efficiency of the estimated models and their suitability for describing the dynamical behaviour of the frame were proved. Then, the magnitudes' part, which represents the Frequency Response Function (FRF) were utilized to construct the mobility matrix (H), while the phases' part were used to plot the modes shapes of the frame. Due to the rectangular shape of (H), the singular value decomposition (SVD) method was adopted to identify how many significant eigenvalues exist and plot the Complex Mode Indicator Function (CMIF) for the complete frame. Three damage indices were adopted to evaluate the state of damage in the frame, namely: frequency, modal damping, and Modes Shapes.

Overall, this article is structured as it follows. Section 2 outlines the article's methodology, while in Section 3, a numerical example was provided to demonstrate the application of the ARMAX model for damage detection. Finally, the conclusions were drawn in Section 4.

## 2. METHODOLOGY

There are a lot of categories of damage detection methods, according to the technique utilized to identify the damage from the measured data. Valuable information about damage detection methods, their levels, and damage indicators are available in references [32, 8, 16; 39, 43; 30; 7; 46; 49; 45]. Frequency's changes method will be adopted in the current paper, since shifts in natural frequencies were widely used to detect damage in structures. This method mainly depends on the concept that variations in the structural properties will result in alterations in the vibration frequencies and amplitudes. In spite of the significant practical limitations of this method [16, 43], it has been utilized by many researchers to detect damage, especially in applications where the frequency shifts can be measured very precisely or there is an expectation of large levels of damage, and thus in the current approach, it was assumed that these two conditions were applicable in the current research effort. Figure 1 depicts the overall methodology proposed throughout this article for damage identification and localization.

First of all, a  $n$ -story shear frame is simulated, in the following scenarios and cases:

$$S_{sj} \text{ with } sj = 1, \dots, s_n$$

where  $S_{sj}$  represents the damage scenario and  $s_n$  is the number of damage scenarios considered.

$$S_{cj}, cj = 1, \dots, c_m$$

where  $C_{cj}$  is the damage cases and  $c_m$  represents the number of damage cases considered for each of damage scenarios. Moreover,  $u(t)$  is the excitation,  $y(t)_i, i=1, \dots, k$  is the response of the building at the  $k_i$  location, where  $y(t)_i$  represents the output and  $k$  is the total number of measurement points.

Then, the responses of the frame (assumed as measurements), due to each one of the damage cases, will be utilized to obtain the transfer functions of the frame by the ARMAX parametric model, while considering the frame as a linear system for all the measurement points (sensors), as it will be presented in the following subsection.

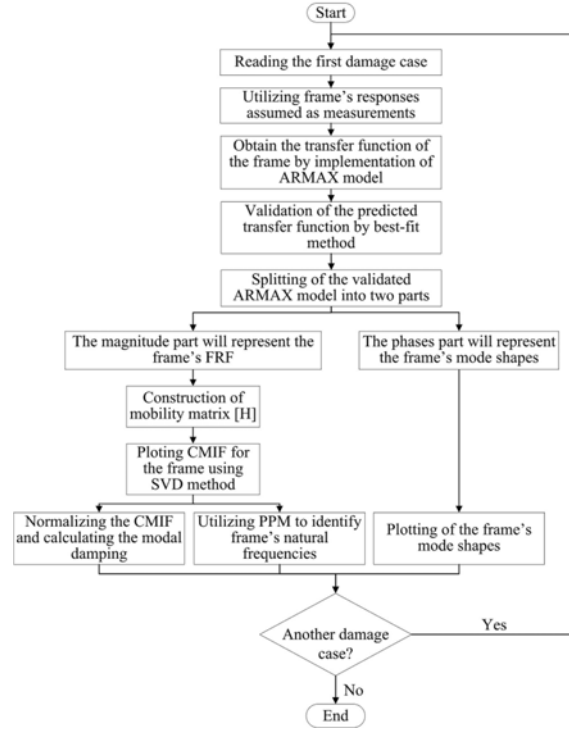


Fig. 1. Proposed damage diagnosis scheme

### 2.1. ARMAX model structure and estimation

A typical dynamic system is presented at Figure 2, subjected to input  $u(t)$  and the response of the system to be described by the output  $y(t)$ , which is affected by the disturbance  $v(t)$ . It is worth mentioning that the disturbance cannot be controlled and even the input may be unknown and uncontrollable in some kind of systems.

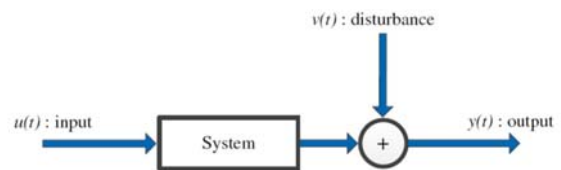


Fig. 2. A dynamic system with input  $u(t)$ , output  $y(t)$  and disturbance  $v(t)$

According to whether the excitation of the structural system is measured or not, and the excitation type (stationary, impulse or step), the parametric model structures can be divided into two main categories [3]: a) model structures for stochastic input, and b) model structures for deterministic input. Eq. 1 below denotes the general input/output model structure for modeling of linear and time-invariant dynamic systems, excited by a deterministic input:

$$y(t) = G(q)u(t) + H(q)e(t) \quad (1)$$

where  $G(q)$  and  $H(q)$  are the transfer functions of the

deterministic part and the stochastic part respectively,  $u(t)$  represents the input signal,  $y(t)$  is the output signal and  $e(t)$  is the white noise (equation error). The parameters in the transfer function in Eq. (1) are determined during the system identification process. The vector  $\theta$  is usually utilized to designate these parameters and the system description given in Eq. (1) can be rewritten in the following form:

$$y(t)=G(q, \theta)u(t)+H(q, \theta)e(t) \quad (2)$$

The Auto-Regressive Moving Average with External input ARMAX model is one of many different approaches that are available to solve Eq. (2) in terms of  $\theta$  as presented in the sequel. The ARMAX model used in this study is a Single Input Single Output (SISO) ARMAX model, since only one source of excitation is used to excite the structure. Generally, the simple relation between the input and output is provided by the following linear difference equation:

$$y(t)+a_1y(t-1)+\dots+a_ny(t-n_a)=b_1u(t-1)+\dots+b_nu(t-n_b)+e(t) \quad (3)$$

Clearly, Eq.(3) has limited capability in defining the disturbance term since it describes the white noise as a discrete error. The ARMAX models overcome this problem by defining the error as a Moving Average (MA) of white noise as presented in Eq.(4):

$$y(t)+a_1y(t-1)+\dots+a_ny(t-n_a)=b_1u(t-1)+\dots+b_nu(t-n_b)+e(t)+c_1e(t-1)+\dots+c_nce(-n_c) \quad (4)$$

The vector  $\theta$  of adjustable parameters can be now formulated in the following form:

$$\theta=[a_1 \dots a_n a b_1 \dots b_n c_1 \dots c_n]^T$$

while  $q$  in an equivalent polynomial form can be denoted as:

$$A(q)y(t)=B(q)u(t)+C(q)e(t) \quad (5)$$

with the following polynomial definitions:

$$A(q)=1+a_1q^{-1}+\dots+a_nq^{-n_a}, B(q)=b_1q^{-1}+\dots+b_nq^{-n_b}, C(q)=1+c_1q^{-1}+\dots+c_nq^{-n_c}$$

and  $n_a$ ,  $n_b$ ,  $n_c$  are the maximum orders of the corresponding polynomial, which are usually determined by an extended trial-and-error process. In Eq.(5), the Moving Average (MA) part is given by  $C(q)e(t)$ . while, Eq. (5) is equivalent to Eq. (2) with

$$G(q, \theta)=(B(q))/(A(q)), H(q, \theta)=(C(q))/(A(q))$$

There are several optimization methods available to obtain the optimal estimate of  $\theta$  by minimizing the disturbance. More details about these methods and their full derivations can be found in [26, 42, 40, 41]. In this work, Gauss-Newton method has been utilized to optimize the mean square value of the prediction error when searching for the optimal ARMAX-model. This searching process is iterative and might converge to a local minimum rather than a global minimum. For this reason, the validation of the estimated model is crucial, and it is allowed to use the estimated model if it passed the validation test. By determining the coefficients of the vector  $\theta$ , the transfer function of the building will be known, and thus the modal parameters of the system will be derived directly from the coefficients.

In this study, the correctness of the estimated models will be validated using the Matlab's best-fit method, according to the following equation [26], which provides an indication about the estimated model's efficiency to represent the main system dynamics (in time domain) and whether the linear simulation is appropriate.

$$Fit = 100 * \left( 1 - \frac{\|y(t)_h - y(t)\|}{\|y(t) - \bar{y}(t)\|} \right)$$

In this equation,  $y(t)$  represents the real output,  $\bar{y}(t)$  is the sample mean, and  $y(t)_h$  represents the output obtained from the identified model. In the sequel, the magnitudes and phases of each one of the estimated transfer functions of the ARMAX models will be extracted.

$$Mag_{(i)}, i=1, \dots, k$$

$$Phz_{(i)}, i=1, \dots, k$$

where  $Mag_{(i)}$  represents the magnitude part for each measurement point,  $Phz_{(i)}$  is the phase part for each measurement point, and  $k$  is the total number of measurement points. The magnitudes' part, which represents the FRF will be utilized to construct the measurements' matrix, i.e. mobility matrix ( $Hmag$ ), while the phases' part will be used to plot the mode shapes ( $PHZ$ ) of the frame as shown in the sequel:

$$Hmag_{(n_f; n_{mf})} = [Mag_{(1;1)} \dots Mag_{(1; n_{mf})} \dots Mag_{(n_f; 1)} \dots Mag_{(n_f; n_{mf})}]$$

$$PHZ_{(n_f; n_{mf})} = [phz_{(1;1)} \dots phz_{(1; n_{mf})} \dots phz_{(n_f; 1)} \dots phz_{(n_f; n_{mf})}]$$

where  $n_f$  is the numbers of floors, and  $n_{mf}$  is the number of measurement points per floor. For instance, in the case study given in Section 3, each one of the element  $Mag$ , in the above mentioned equation, contains one FRF column vector of length 100 (as it resulted from the FRF estimation process).  $Hmag$  includes the FRF columns vectors, corresponding to all the measurement points in each floor (11 measurement points) and for all the buildings floors starting from the zero level to the 10th level (11 levels), and thus the total dimension of  $Hmag$  is (100,121). The same thing is applicable for the  $PHZ$  equation. Since there are unique responses for each measurement location and single excitation,  $H$  will have a rectangular shape, thus the SVD method was adopted to identify how many significant eigenvalues exist and plot the CMIF curve for the frame [5]:

$$CM=SVD(H)$$

where  $CM$  denotes the CMIF curve. The basic assumption for all the Single Degree Of Freedom (SDOF) methods for modal analysis is that at the proximity of resonance, the FRF will be dominated by that vibration mode and the contributions of other vibration modes can be neglected. Based on this assumption, the FRF from a real structure with Multi Degree Of Freedom (MDOF) can be considered as a FRF from a SDOF system [31, 17]. Moreover, the peak-picking method can be utilized to identify the frames natural frequencies, since this method is able to search for peaks by stepping through the CMIF curves, and when the curves have reached a

maximum, it will indicate a new frequency by utilizing the following equation:

$$|CM_{(\omega)}|_{\max} \Rightarrow \omega_r = \omega_{peak}$$

where  $\omega$  represents the identified natural frequency for the mode number  $r$ . After that, the search for the next peak corresponding for the next mode will start and so on. Thus, the method will take into accounts the damage influenced by higher vibration modes.

According to [13] the CMIF curves were normalized so that their magnitudes at zero frequencies are unity. Thus, the values of modal damping will be determined from the normalized CMIF curves denoted as:

$$CM_{(nor)} = CM = CM_{(\omega=1)}$$

## 2.2. Transfer function estimation

In this subsection, the transfer function in terms of the magnitude and the derivation of the amplification factor, utilized for modal damping calculations are presented. Based on the assumption of applicability of the SDOF behaviour [31, 17] mentioned in the previous subsection, and according to Newton's second law, the time domain equation of motion for a single degree of freedom system can be given by [11]:

$$M\ddot{x}(t) + C\dot{x}(t) + Kx(t) = f(t) \quad (6)$$

where  $M$ ,  $C$ , and  $K$  represent the mass, damping, and stiffness values correspondingly, while  $\ddot{x}(t)$ ,  $\dot{x}(t)$ , and  $x(t)$  represent the acceleration, velocity, and displacement and the excitation force is  $f(t)$ . The equivalent frequency domain equation of motion can be obtained using the Laplace transform of Eq.(6) assuming all initial conditions are zero [9]:

$$[Ms^2 + Cs + K]X(s) = F(s) \quad (7)$$

Where  $X(s)$  is the displacement Laplace transform and  $F(s)$  is the force Laplace transform, while Eq. (7) can be rearranged as:

$$H(s) = \frac{X(s)}{F(s)} = \left[ \frac{1}{Ms^2 + Cs + K} \right]$$

The transfer function  $H(s)$  is a complex valued, so it has two parts; a magnitude and a phase. The Frequency Response Function (FRF) can be obtained by substituting the values of the transfer function along the frequency axis ( $j\omega$ -axis) as in the sequel [19]:

$$[H(s)]_{s=j\omega} = [H(\omega)],$$

$$\text{or } [H(\omega)] = \left[ \frac{1}{-\omega^2 M + j\omega C + K} \right] = \left[ \frac{1/M}{-\omega^2 + j\omega C/M + K/M} \right] \quad (8)$$

According to [11],  $C/M=2\xi\omega_n$  where  $\omega_n$  is the natural frequency (radians/sec), and  $\xi$  is the damping ratio, while (8) becomes:

$$[H(\omega)] = 1/M \left[ \frac{1}{-\omega^2 + j\omega 2\xi\omega_n + \omega_n^2} \right]$$

which can be formulated as:

$$[H(\omega)] = 1/M \left[ \frac{1}{(\omega_n^2 - \omega^2) + j(2\xi\omega\omega_n)} \right] \quad (9)$$

$$[H(\omega)] = 1/M \left[ \frac{1}{\sqrt{(\omega_n^2 - \omega^2)^2 + j(2\xi\omega\omega_n)^2}} \right]$$

Substituting for  $M = \omega_n^2 / K$  [11] in Eq.(9) yields the transfer function in terms of the magnitude:

$$[H(\omega)] = [1/K] \left[ \frac{\omega_n^2}{\sqrt{(\omega_n^2 - \omega^2)^2 + j(2\xi\omega\omega_n)^2}} \right] \quad (10)$$

## 2.3. Modal parameters estimation

In the presented work, the Magnification-Factor method was utilized to calculate the modal damping. According to this method, the peak value for the magnitude of the frequency response function happens when the denominator of Eq.(10) is minimum [13] or the derivative of Eq.(10) is set to zero as shown below:

$$\frac{d}{d\omega} \left[ (\omega_n^2 - \omega^2)^2 + 4\xi^2 \omega^2 \omega_n^2 \right] = 0 \quad (11)$$

The solution of Eq.(11) for  $\omega$ , is called the resonant frequency  $\omega_r$  and is being calculated by:

$$\omega_r = \sqrt{1 - 2\xi^2} \omega_n \quad (12)$$

Finally, substituting Eq.(12) in Eq.(10) gives the magnitude of the frequency response function at the resonant frequency given in the sequel, which is called the amplification factor  $Q$ .

$$Q = \frac{1}{\sqrt{2\xi\sqrt{1-\xi^2}}} \quad (13)$$

The phases part, previously described in section (2.1), will be used to plot the mode shapes (PHZ) of the frame.

## 3. SIMULATION RESULTS

In the current research, a regular building's steel frame has been utilized as a case study. The frame is for a ten story bench mark building 45.75m by 45.75m in plan and 40.82m in elevation with one underground level. This bench mark building was proposed and designed by the SAC project for the Los Angeles, USA [35]. The lateral load-resisting system is composed from four steel perimeter moment-resisting frames. The bays are 9.15 m on center, in both directions.

The floor-to-floor height is 3.65 m for the underground floor, 5.49 m for the ground floor and 3.96 m for the remaining eight stories. Figure 3 shows the building elevation. The lumped seismic mass for each story was applied at the center of each level.

Table 1 displays seismic masses for each story and the steel sections used for the beams and columns. In this Table 1, the code  $W(\times\omega t)$  refers to the nominal size of wide flange structural steel section with, I or H shape. The nominal depth of the section in (inch) is referred by ( $d$ ), while (wt) refers to the section weight per unit length ( $lb/ft$ ). The

analysis was conducted based on a pinned support condition assumption at the bottom of the underground floor, which is also prevented from side movement as it is shown in Figure 3.

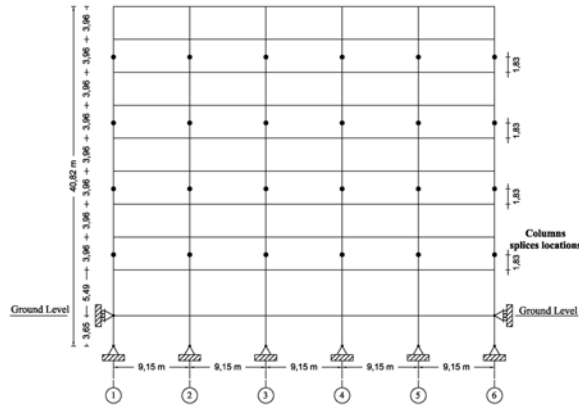


Fig. 3. Building's elevation

Abaqus 6.12 [14] finite-element software was utilized to perform the time history analysis for the frame. The obtained responses at 110 different locations (assumed as a sensors) corresponds to the ends of columns and mid of beams were assumed as measurements. Quadratic elements types (B22) from Abaqus's beam library were used for simulating the structural behavior of beams and columns. A horizontal ground acceleration in the form of a normally distributed Gaussian white noise excitation with zero mean and a unitary variance was used to excite the model.

Table 1: Sections dimensions and properties of the building

Levels	Beams Sections	Columns Sections	Seismic mass (kg)
Ground	W36 × 160	W14 × 500	$9:65 \times 10^5$
1 <sup>st</sup>	W36 × 160	W14 × 500	$1:01 \times 10^6$
2 <sup>nd</sup>	W36 × 160	W14 × 500	$9:89 \times 10^5$
3 <sup>rd</sup>	W36 × 135	W14 × 455	$9:89 \times 10^5$
4 <sup>th</sup>	W36 × 135	W14 × 455	$9:89 \times 10^5$
5 <sup>th</sup>	W36 × 135	W14 × 370	$9:89 \times 10^5$
6 <sup>th</sup>	W36 × 135	W14 × 370	$9:89 \times 10^5$
7 <sup>th</sup>	W30 × 99	W14 × 283	$9:89 \times 10^5$
8 <sup>th</sup>	W27 × 84	W14 × 283	$9:89 \times 10^5$
9 <sup>th</sup>	W24 × 68	W14 × 257	$9:00 \times 10^6$

The amplitude of the Gaussian white-noise signal, in the time domain, was scaled by a factor of 0.3g. The total simulation time was 60 seconds, with a simulation time step of 0.02 seconds. The frequency bandwidths of the excitation and of the obtained signals have been 25 Hz, which were equal to one-half of the sampling frequency.

The damage in the frame was simulated by reducing the Modulus of elasticity  $E$  for specific columns by 75% of the undamaged ones. The value of  $E$  for the healthy columns was 203.9 GPa, while for the damaged columns was 50.9 GPa. Two scenarios were assumed for damages in the frame, damage scenario no.1 consist of increasingly destroying the columns of the ground floor, while for damage scenario no.2, the damage locations were changed by destroying column no.1 in a floor, and this was repeated for five stories. Table 2 summarizes the assumed damage scenarios.

The transfer function of the frame has been derived by utilizing the ARMAX parametric model and considering the frame as a linear system for all measurement points (sensors). Since the orders of the ARMAX model were determined by a trial-and-error process, many trials with different combinations of the factors ( $n_a$ ,  $n_b$ ,  $n_c$ , and  $n_k$ ) were examined to obtain the highest possible best-fit result, which is considered one of the best methods to guarantee that the estimated transfer function can effectively describe the dynamic behavior of the system. Thus, the orders of the polynomials  $n_a$ ,  $n_b$ ,  $n_c$ , and  $n_k$  for the healthy, damage scenario no.1, and damage scenario no.2 were 40, 40, 40, 1, 42, 42, 42, 1 and 40, 40, 40, 1 respectively. To validate the correctness of the estimated models, the Matlab best-fit method has been implemented. Fig. 4 displays the best-fit results, which clearly prove the efficiency of the estimated models and their suitability for further usage.

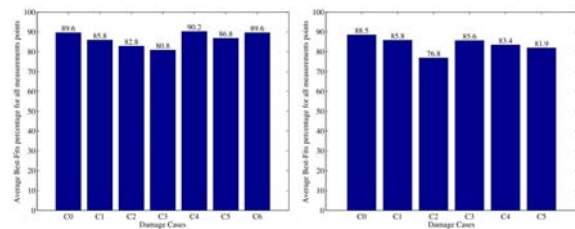


Fig. 4. Efficiency of estimated ARMAX models in term of Best-Fit results

Table 2: Frame damage scenarios

Damage Scenario No.1	Damage Scenario No.2
C0: No damage case	C0: No damage case
C1: Col. No.1 - ground floor	C1: Col. No.1 - ground floor
C2: Cols. No.(1 & 2) - ground floor	C2: Col. No.1 - 1st floor
C3: Cols. No.(1 & 2 & 3) - ground floor	C3: Col. No.1 - 2nd floor
C4: Cols. No.(1 & 2 & 3 & 4) - ground floor	C4: Col. No.1 - 3rd floor
C5: Cols. No.(1 & 2 & 3 & 4 & 5) - ground floor	C5: Col. No.1 - 4th floor
C6: Cols. No.(1 & 2 & 3 & 4 & 5 & 6) - ground floor	

### 3.1. Frequency

The identified frequencies for all cases of damage scenarios are presented in the CMIF curves of Figure 5 and Figure 6. The present work has been restricted to investigate the first five modes. The first five frame natural frequencies, obtained from Abaqus's frequency analysis and based on the frame mathematical model are: 0.4428, 1.1798, 2.0314, 3.0493 and 4.1986 Hz. The first five identified natural frequencies, based on the assumed measurements, for the healthy case of the frame are: 0.379, 1.14, 2.02, 3.03 and 4.17 Hz, which are very close to the frame natural frequencies obtained from Abaqus's frequency analysis.

As it has been depicted in Figures 5 and 6, the comparison between the identified natural frequencies clearly indicated the existence of damage due to the sharp increase in the amplitudes (resonance) of the CMIF curves. For the damage scenario no.1, it is obvious from Figure 7 that the increase of damage caused a decrease (shift) in natural frequencies, while the change in damage locations for damage scenario no.2 did not affect the resonances absolutely as it was depicted in Figure 8. There are two possible reasons to explain the failure of the proposed damage identification procedure for damage detection of damage scenario no.2. Firstly, due to the professional design of this bench mark building, the redistribution of the stresses and forces in the frame overcome the damage. In this case, the different members of the frame worked effectively to compensate for the deficiency of the frame in resisting the excitation due to the damage existence at a specific member and at a specific floor. Secondly, the level of damage for scenario no.2 is not so large to be identified by the frequency's changes method.

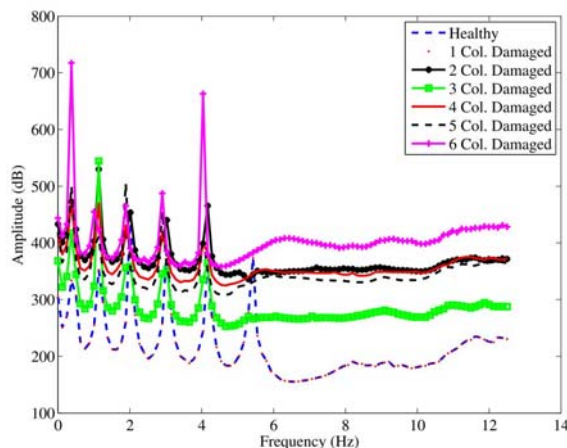


Fig. 5. Comparison of CMIF curves estimated from the mobility matrix (H) for all damage cases of damage scenario no. 1

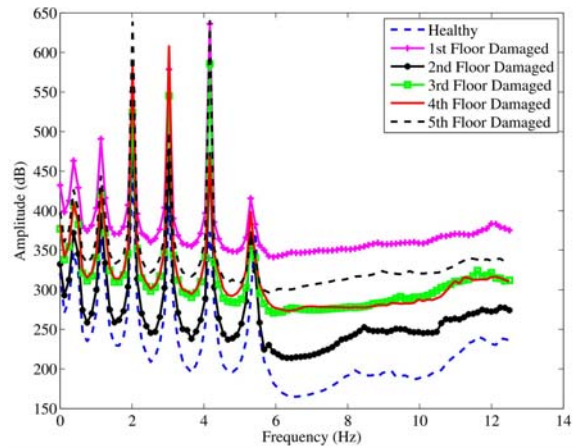


Fig. 6. Comparison of CMIF curves estimated from the mobility matrix (H) for all damage cases of damage scenario no. 2

### 3.2. Damping

The damage in the frame can also be identified from the amplitudes of vibrations of CMIF curves. The amplitudes of vibrations of the damage scenarios no.1 and no.2 are shown in Figure 9 and 10 respectively, where it is clearly indicated an increase in the vibration amplitudes as a general trend. This indicates also that the damping effects are considerably decreased so that the amplitude can increase.

In order to find the values of modal damping, the CMIF curves were normalized so that their magnitudes at zero frequencies are unity. Afterwards, the modal damping values were calculated using Eq. (13). The results of the damage scenarios no.1 are depicted in Figure 11. It is obvious that the general trend (apart of mode 3) is a decrease in the modal damping. The reader should distinguish between modal damping and the overall damping of the structure, which exhibit marked non-linearity, for more details see [12, 38]. This decrease in modal damping reflects the increase in the damage's size of the frame and it was vanished for some frequencies of damage cases C4, C5, C6 and C7. In the case of the damage scenario no.2, Figure 12 shows that there is a slight increase in the modal damping for the first two vibration modes, while there is a clear decrease in modal damping for the higher modes. It can be concluded that the general trend for vibration amplitudes and modal damping can be considered as an index for detecting the increase or decrease in the damage size, but this effect will not provide any further information about damage locations.

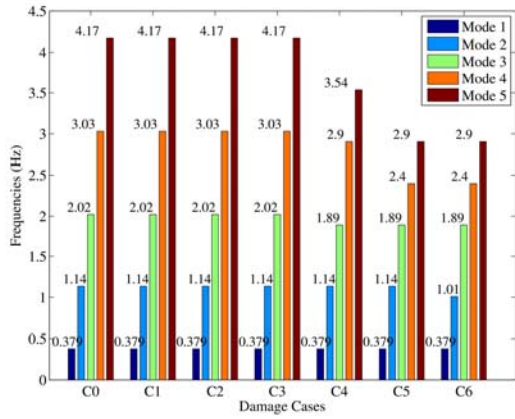


Fig. 7. The 1st five natural frequencies identified in the damage scenario no. 1

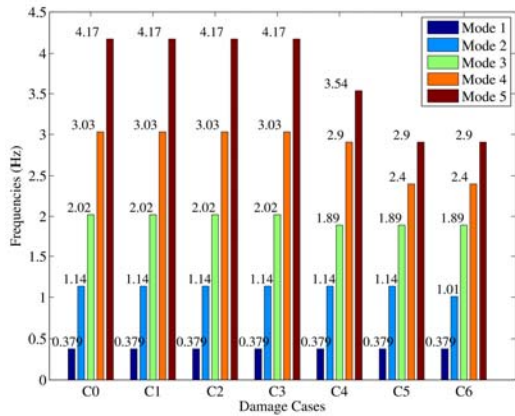


Fig. 8. The 1st five natural frequencies identified in the damage scenario no.2

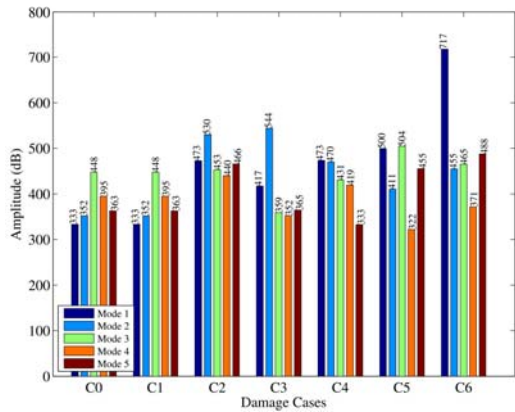


Fig. 9. Amplitudes of identified natural frequencies for the damage scenario no. 1

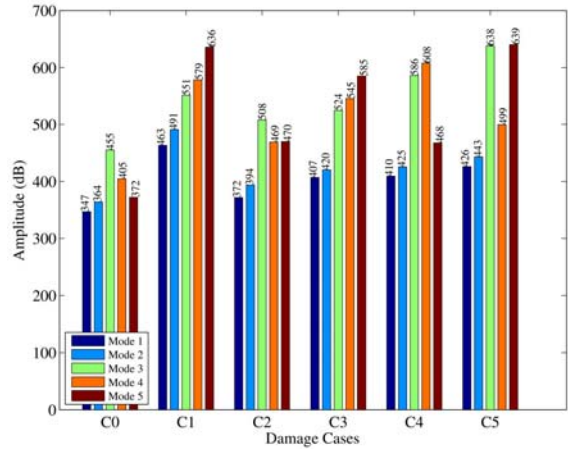


Fig. 10. Amplitudes of identified natural frequencies for the damage scenario no. 2

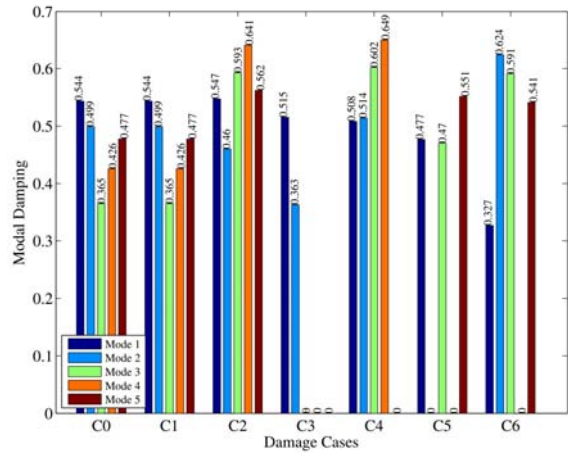


Fig. 11. Modal damping for the damage scenario no.1

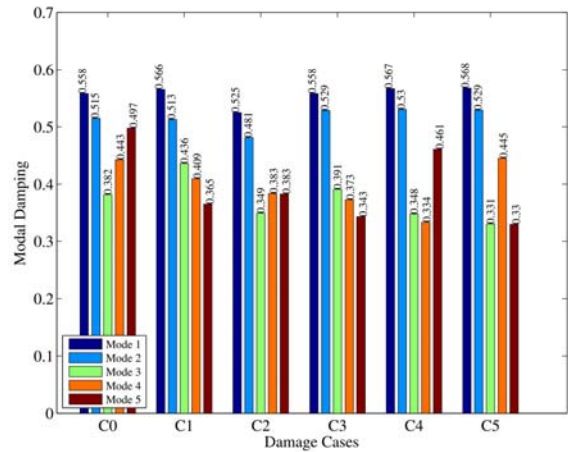


Fig. 12. Modal damping for the damage scenario no. 2



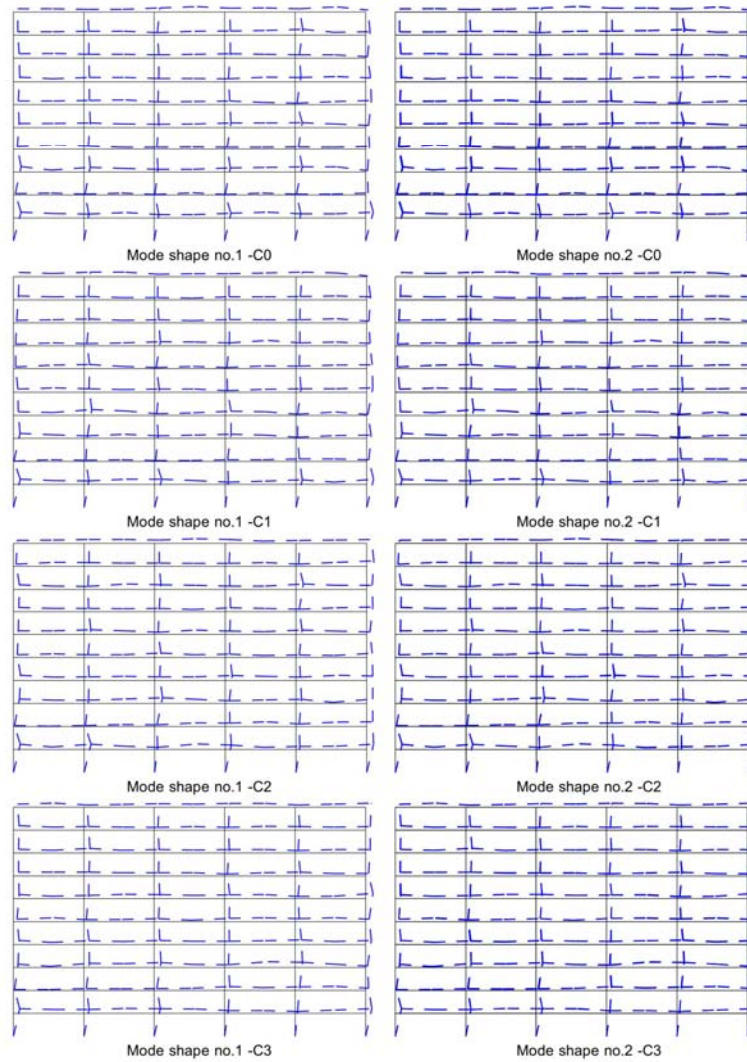


Fig. 13. Vibration mode shapes of the frame in the case of damage scenario no. 1

### 3.3. Modes Shapes

Fig. 13 and 14 depict the first two mode shapes of the frame for each damage case of damage scenario no.1 as they were identified from the measurements. Visual inspection for these modes shapes reveals the locations of damage in the frame. Clearly, the deformed shape of the beams at the first floor level (assumed damage locations) tends to be more flattening as the damage increases from case C0 to case C6 for the two mode shapes. In other words, it is possible to expect damage locations at the points (sensors) where the difference in the phase is the least (for successive different monitoring cases). For the damage scenario no.2, shown in Fig. 15 and Fig. 16, even that it looks that the points of assumed damage have the least differences in the phase, it is difficult to specify damage locations exactly due to the small damage size in each floor.

### 4. CONCLUSIONS

In this article, the Auto-Regressive Moving Average with eXternal input ARMAX model was

successfully utilized for the construction of FRF, based on Abaqus's simulation results. The identified frame's natural frequencies were very close to the theoretical ones obtained from Abaqus's frequency analysis. Sharp increases in the amplitudes of the CMIF curves revealed the existence of damage in the frame. Furthermore, it can be concluded that the general trend for vibration amplitudes and modal damping can be considered as an index for detecting the increase or decrease in the damage size, but it is not able to give any information about damage locations, while visual inspection for modes shapes reveals the locations of damage in the frame.

In the future, the authors are planning for further development and evaluation of the proposed methodology to include the detection of damage up to levels 3 and 4. One recognizable drawback is that this method does not manage closely spaced modes, while it is possible to expect damage locations at the points (sensors) where the difference in the phase is the least (for successive different monitoring cases).

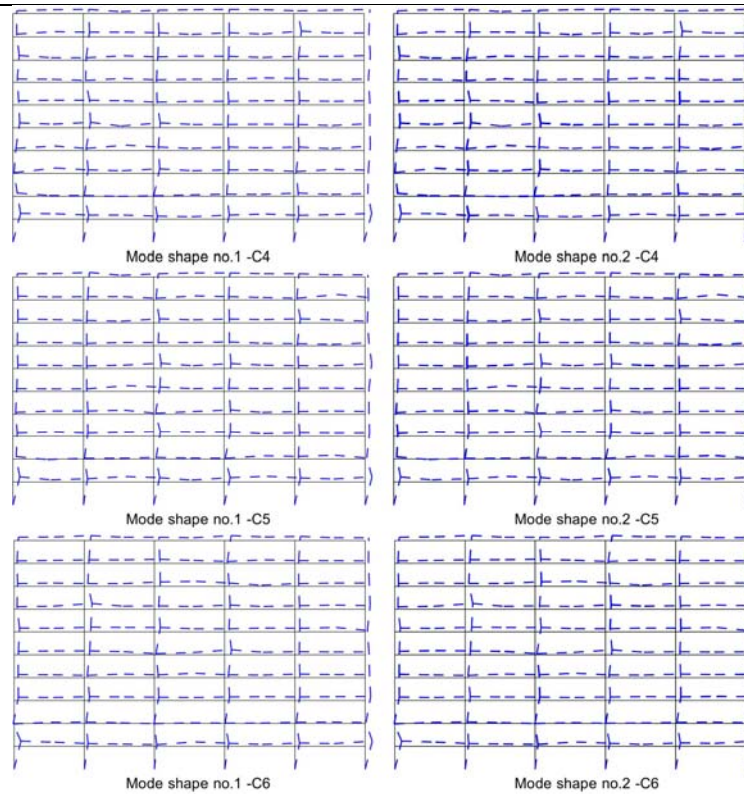


Fig. 14. Vibration mode shapes of the frame in the case of damage scenario no. 1

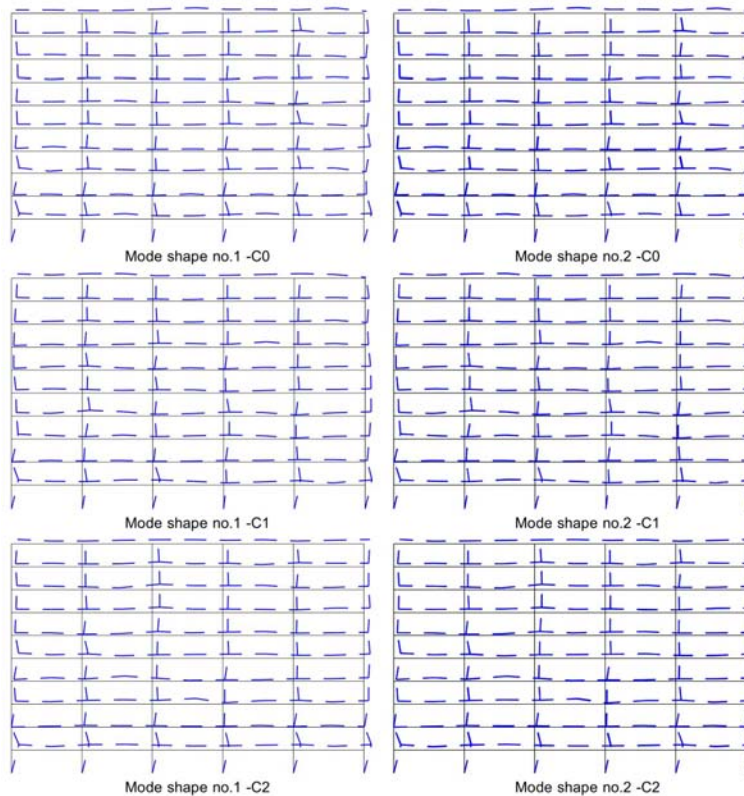


Fig. 15. Vibration mode shapes of the frame in the case of damage scenario no. 2

## 5. ACKNOWLEDGEMENTS

The first author would like to acknowledge the Ministry of Higher Education and Scientific Research - University of Mosul-Iraq for the PhD scholarship provided by them.

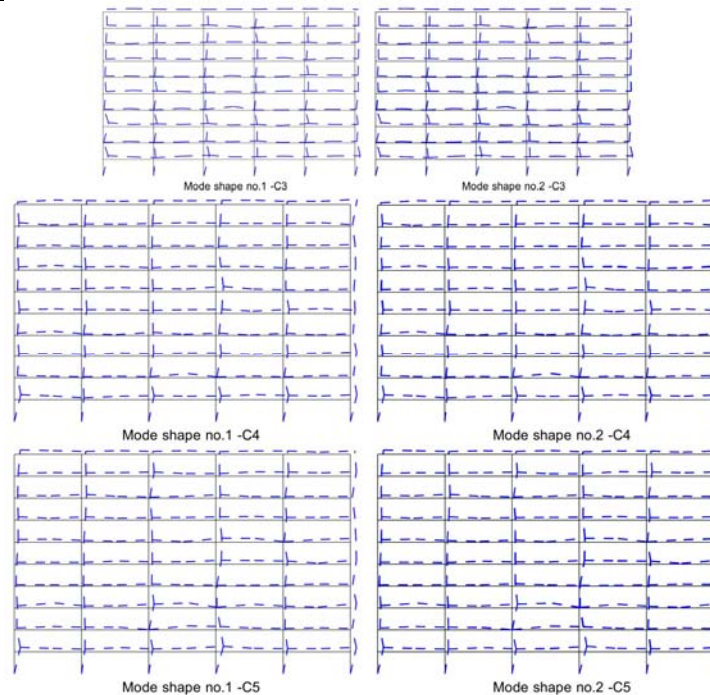


Fig. 16. Vibration mode shapes of the frame in the case of damage scenario no. 2

## REFERENCES

- Aktan A.E., Ellingwood B.R., Kehoe B. Performance-based engineering of constructed systems 1. *Journal of structural engineering*, 133(3): 311-323, 2007.
- Alvin K.F., Robertson A.N., Reich G.W., Park K.C. Structural system identification: from reality to models. *Computers & structures*, 81(12):1149-1176, 2003.
- Andersen P. Identification of civil engineering structures using vector ARMA models. PhD thesis, Aalborg University, Denmark, 1997.
- Astrom K. J., Eykhoff P. System identification a survey. *Automatica*, 7(2):123-162, 1971.
- Avitabile P. Can you explain the complex mode indicator function (cmif) again? what are these crossover frequencies? *Experimental Techniques*, 37(2):3-5, 2013.
- Bodeux J.B., Golinval J.C. Application of armav models to the identification and damage detection of mechanical and civil engineering structures. *Smart Materials and Structures*, 10(3):479, 2001.
- Boller C., Chang F.K., Fujino Y.. *Encyclopedia of structural health monitoring*. John Wiley, 2009.
- Capecchi D., Vestroni F. Monitoring of structural systems by using frequency data. *Earth- quake engineering & structural dynamics*, 28(5):447-461, 1999.
- Catbas F.N., Brown D.L., Aktan A.E. Use of modal flexibility for damage detection and condition assessment: case studies and demonstrations on large structures. *Journal of Structural Engineering*, 132(11):1699-1712, 2006.
- Catbas F.N., Kijewski-Correa T., Aktan A.E. Structural identification (st-id) of constructed facilities: Approaches, methods and technologies for effective practice of st-id. In *Am Soc Civ Eng*, 2011.
- Chopra A.K. *Dynamics of structures*, volume 3. Prentice Hall New Jersey, 1995.
- Chowdhury I., Dasgupta S.P. Computation of rayleigh damping coefficients for large systems. *The Electronic Journal of Geotechnical Engineering*, 8(0), 2003.
- da Silva S., Dias M. J., Lopes V. J., Brennan M. J. Structural damage detection by fuzzy clustering. *Mechanical Systems and Signal Processing*, 22(7):1636-1649, 2008.
- Dassault Systemes. *Abaqus/cae users manual*, version 6.12-1. Pawtucket (RI), 2012.
- De Silva C.W. *Vibration: fundamentals and practice*. CRC press, 2006.
- Doebbling S.W., Farrar C.R., Prime M.B., Shevitz D.W. *Damage identification and health monitoring of structural and mechanical systems from changes in their vibration characteristics: a literature review*. Technical report, Los Alamos National Lab., NM (United States), 1996.
- Fu Z.F., He J. *Modal analysis*. Butterworth-Heinemann, 2001.
- Hart G.C., Yao J.T.P. System identification in structural dynamics. *Journal of the Engineering Mechanics Division*, 103(6):1089-1104, 1977.
- Inc. Vibrant Technology. *Integration and differentiation of frfs*. Technical report, <http://www.vibetech.com>, 2006.
- Kampas G., Makris N. Modal identification of freeway overcrossings with soil-structure interaction: a case study. *Structural Control and Health Monitoring*, 20(3):304-319, 2013.
- Lee C.G., Yun C.B. Parameter identification of linear structural dynamic systems. *Computers & structures*, 40(6):1475-1487, 1991.
- Li H., Deng X., Dai H. Structural damage detection using the combination method of emd and wavelet analysis. *Mechanical Systems and Signal Processing*, 21(1):298-306, 2007.
- Liu S.C., Yao J.T.P. Structural identification concept. *Journal of the Structural Division*, 104 (12):1845-1858, 1978.
- Liu T.Y., Chiang W. L., Chen C. W., Hsu W. K., Lin . C. W., Chiou D. J., Huang P. C. Structural system identification for vibration bridges using the Hilbert-Huang transform. *Journal of Vibration and Control*, 18(13):1939-1956, 2012.
- Liu T.Y., Chiang W.L., Chen C.W., Hsu W.K., Lu L.C., Chu T.J. Identification and monitoring of bridge health from ambient vibration data. *Journal of Vibration and Control*, 17(4):589-603, 2011.
- Ljung L. *System Identification Toolbox for Use with {MATLAB}*. The MathWorks, Inc., 2012.
- Ljung L. *System identification: theory for the user*. Information and System Sciences Series. Prentice-Hall, Englewood Cliffs, New Jersey, 7632, 1987.
- Loh C.H., Weng J.H., Chen C.H., Lu K.C. System identification of midstory isolation building using both

- ambient and earthquake response data. *Structural Control and Health Monitoring*, 20(2):19-35, 2013.
29. Minami Y., Yoshitomi S., Takewaki I. System identification of super high-rise buildings using limited vibration data during the 2011 tohoku (japan) earthquake. *Structural Control and Health Monitoring*, 20(11):1317-1338, 2013.
  30. Montalvao D., Maia N.M.M., Ribeiro A.M.R. A review of vibration-based structural health monitoring with special emphasis on composite materials. *Shock and Vibration Digest*, 38(4):295-326, 2006.
  31. Nagarajaiah S., Basu B. Output only modal identification and structural damage detection using time frequency & wavelet techniques. *Earth-quake Engineering and Engineering Vibration*, 8(4):583-605, 2009.
  32. Nakamura M., Masri S.F., Chassiakos A.G., Caughey T.K. A method for nonparametric damage detection through the use of neural networks. *Earthquake engineering & structural dynamics*, 27(9):997-1010, 1998.
  33. National Instruments Corporation. Selecting a model structure in the system identification process. Technical report, <http://www.ni.com/whitepaper/4028/en/>, 2010.
  34. Oates R. Armax for system identification. Nottingham University Lecture, 2011.
  35. Ohtori Y., Christenson R.E., Spencer B.F.Jr., Dyke S.J. Benchmark control problems for seismically excited nonlinear buildings. *Journal of Engineering Mechanics*, 130(4):366-385, 2004.
  36. Pan Q. System identification of constructed civil engineering structures and uncertainty. PhD thesis, Citeseer, 2007.
  37. Petsounis K.A., Fassois S.D. Parametric time-domain methods for the identification of vibrating structures a critical comparison and assessment. *Mechanical Systems and Signal Processing*, 15(6):1031-1060, 2001.
  38. Richardson M.H. Derivation of mass, stiffness and damping parameters from experimental modal data. Hewlett Packard Company, Santa Clara Division, 1977.
  39. Rytter A. Vibration Based Inspection of Civil Engineering Structures, 1993. PhD thesis, Ph. D. dissertation, 1993.
  40. Safak E. Identification of linear structures using discrete-time filters. *Journal of Structural Engineering*, 117(10):3064-3085, 1991.
  41. Saito T., Yokota H. Evaluation of dynamic characteristics of high-rise buildings using system identification techniques. *Journal of wind engineering and industrial aerodynamics*, 59(2):299-307, 1996.
  42. Soderstrom T., Stoica P. System identification. Prentice-Hall, Inc., 1988.
  43. Sohn H., Farrar C.R., Hemez F.M., Shunk D.D., Stinemates D.W., Nadler B.R., Czarnecki J.J. A review of structural health monitoring literature: 1996-2001. Los Alamos National Laboratory Los Alamos, NM, 2004.
  44. Tang J.P., Chiou D.J., Chen C.W., Chiang W.L., Hsu W.K., Chen C.Y., Liu T.Y. A case study of damage detection in benchmark buildings using a hilbert-huang transform-based method. *Journal of Vibration and Control*, 17(4):623-636, 2011.
  45. Thu H.H., Mita A. Assessment and evaluation of damage detection method based on modal frequency changes. In *SPIE Smart Structures and Materials+ Nondestructive Evaluation and Health Monitoring*, pages 86923M-86923M. International Society for Optics and Photonics, 2013.
  46. Xia Y. System Identification and Damage Detection of Nonlinear Structures, 2011. PhD thesis, University of California, Irvine, 2011.
  47. Xia Y., Hao H., Brownjohn J.M.W., Xia P.Q. Damage identification of structures with uncertain frequency and mode shape data. *Earthquake engineering & structural dynamics*, 31(5):1053-1066, 2002.
  48. Xing Z., Mita A. A substructure approach to local damage detection of shear structure. *Structural Control and Health Monitoring*, 19(2):309-318, 2012.
  49. Yang Y.B., Chen C.T., Chang K.C. On applicability of Hilbert-huang transform for vibration analysis of a two-member truss. *The IES Journal Part A: Civil & Structural Engineering*, 5(2):67-78, 2012.
  50. Zanaz A., Yotte S., Fouchal F., Chateaufneuf A. Efficient masonry vault inspection by monte carlo simulations: Case of hidden defect. *Case Studies in Structural Engineering*, 5:1-12, 2016.

Received 2016-07-06

Accepted 2016-09-14

Available online 2016-09-19



#### Tarek Edrees Saeed Alqado

I have received my B.Sc & M.Sc in Civil Engineering – Structures from Mosul University - Iraq in 1992 & 2001 respectively. In the past i have worked as a site engineer for many years. During the period 2006 – 2010 I have been a lecturer for computer applications at Civil Engineering Department at the University of Mosul. In March 2015, I have finished my PhD study at the Department of Civil, Environmental and Natural Resources Engineering at the division of Structural and Construction Engineering, Luleå University of Technology.

My main research interests include fields, such as: Structural Control Systems, System Identification, Earthquake Engineering, Analysis and Design of Structures and Dynamics of Structures.



#### George

#### NIKOLAKOPOULOS

Professor on Robotics and Automation at the Department of Computer Science, Electrical and Space Engineering at Luleå University of Technology, Luleå, Sweden. His work is focusing in the area of Robotics, Control Applications, while he has a significantly large experience in Creating and Managing European

and National Research Projects. In the past he has been working as project manager and principal investigator in Several R&D&I projects funded by the EU, ESA, Swedish and the Greek National Ministry of Research. George is the coordinator of H2020-ICT AEROWORKS project in the field of Aerial Collaborative UAVs and H2020-SPIRE project DISIRE in the field of Integrated Process Control. In 2013 he has established the bigger outdoors motion capture system in Sweden and most probably in Europe as part of the FROST Field Robotics Lab at Luleå University of Technology. In 2014, he has been nominated as LTU's Wallenberg candidate, one out of three nominations from the university and 16 in total engineering nominations in Sweden. In year 2003, George has received the Information Societies Technologies (IST) Prize Award for the best paper that Promotes the scopes of the European IST (currently known as ICT) sector. His publications in the field of UAVs have received top recognition from the related scientific community, while have been several times listed in the TOP 25 most popular publications in Control Engineering Practice from Elsevier. In 2014 he has received the 2014 Premium Award for Best Paper in IET Control Theory and Applications, Elsevier for the research work in the area of UAVs, His published scientific work includes more than 150 published International Journals and Conferences in the fields of his interest.